Joint Channel Estimation and Generalized Approximate Messaging Passing-Based Equalization for Underwater Acoustic Communications

GUANG YANG[1,2], **TAILIAN LIU**[2], **HANXUE DING**[3], **QI YAN**[1], **AND XINJIE WANG**[1]

[1]School of Information and Control Engineering, Qingdao University of Technology, Shandong 266033, China
[2]College of Science and Information Science, Qingdao Agricultural University, Shandong 266109, China
[3]School of Electronic and Information Engineering, Beijing Jiaotong University, Beijing 100044, China

Corresponding author: Tailian Liu (tailian12@163.com)

ABSTRACT Acquiring channel state information and mitigating multi-path interference are challenging for underwater acoustic communications under time-varying channels. We address the issues using a superimposed training (ST) scheme with a least squares (LS) based channel estimation algorithm. The training sequences with a small power are linearly superimposed with the symbol sequences, and the training signals are transmitted over all time, resulting in enhanced tracking capability to deal with time-varying underwater acoustic channels at the cost of only a small power loss. To realize the full potentials of the ST scheme, we develop a LS based channel estimation algorithm with superimposed training, where the Toeplitz matrix is used, which is formed by the training sequences, enabling channel estimation with superimposed training. In particular, a low-complexity channel equalization algorithm based on generalized approximate messaging passing (GAMP) is proposed, where the a priori, a posteriori, extrinsic means and variances of interleaved coded bits are computed, and then convert them into extrinsic log likelihood ratios for BCJR decoding. Its computational complexity is only in a logarithmic order per symbol. Moreover, the channel estimation, GAMP equalization and decoding are performed jointly in an iterative manner, so that the estimated symbol sequences can also be used as virtual training sequences to improve the channel estimation and tracking performance, thereby remarkably enhance the overall system performance. Moving communication experiments in Jiaozhou Bay (communication frequency 12 kHz, bandwidth 6 kHz, sampling frequency 96 kHz, symbol transmission rate 4 ksym/s) were carried out, and the experimental results verify the effectiveness of the proposed technique.

INDEX TERMS Time-varying underwater acoustic channels, superimposed training, generalized approximate messaging passing, iterative turbo receiver.

I. INTRODUCTION

Underwater acoustic communication technology is widely applied in the fields of marine oil resources exploration, underwater rescue, underwater operations, etc. However, the underwater acoustic channel is hostile as the multi-path

The associate editor coordinating the review of this manuscript and approving it for publication was Haiquan Zhao.

interference can be severe, and it is time-varying due to the impact of surface waves, ocean currents, turbulence, etc. When there is the relative motion between the transmitter and the receiver, the channels can drastically change, making it challenging to achieve accurate estimates and reliable equalizations of the time-varying multi-path channels [1]–[3].

Extensive researches have been carried out in the fields of estimation and equalization of time-varying underwater

acoustic channels [4]–[21]. Subspace, compressed sensing, cluster adaptation, orthogonal matching pursuit, sparse and sparse Bayesian learning and so on were proposed to estimate underwater acoustic channels. All the channel estimation algorithms employed traditional time-multiplexing based training, i.e., the training sequences (T. Seq.) are inserted into the data sequences, which results in both spectrum loss and power loss, and it has poor capability of tracing time-varying channels when the channel state informations of the training sequences and the data sequences are inconsistent. In order to address the issues, the superimposed training (ST) scheme is proposed, where the training sequences are linearly superimposed with the symbol sequences, which only brings about a small power loss. The training signals are continuously transmitted, therefore, the capability of tracking time-varying channels can be obviously improved [4]–[15].

Turbo equalization, decision feedback equalization, time reversal mirror equalization, blind equalization and so on were proposed for channel equalization, which are traditional channel equalization algorithms. In contrast to blind equalization algorithms, equalization algorithms based channel estimation have faster convergence rate for time-varying channels. Decision feedback equalization, time reversal mirror equalization and so on can be used with channel estimation to enhance the equalization performance of time-varying channels [4]–[15]. Turbo equalization can be used to achieve remarkable equalization performance gain through the soft information exchange between the equalizer and the decoder. It can be divided into two categories, i.e., turbo equalization based on channel estimation, where channel estimation is embedded in turbo equalization, and direct turbo equalization without channel estimation, where equalizer coefficients can be directly determined based on adaptive algorithms. The first one is more suitable for time-varying channels, as it has faster convergence rate than the second one [16]–[20].

In general, the ST scheme and turbo equalization have potential capability to deal with time-varying channels. To realize the full potentials of the ST scheme, on the basis of the ST scheme, least squares (LS) based channel estimation algorithm is proposed to estimate channels and remove the training interference. In particular, low-complexity channel equalization based on generalized approximate messaging passing (GAMP) is proposed. Unlike traditional turbo equalization (convert the input data into the form of Gaussian variables), GAMP keeps the form of discrete and independent random variables of the input data (interleaved coded bits), and effectively avoid the information loss of the interleaved coded bits, thereby greatly improve the performance of equalization and decoding. Its computational complexity is only in a logarithmic order per symbol. Moreover, the ST scheme, the LS algorithm, and the GAMP algorithm are combined to construct the ST-GAMP technique, and they are performed jointly in an iterative manner (turbo equalization) to remarkably enhance the overall system performance. Field

experiments were carried out in Jiaozhou Bay in 2019, and the experimental results verify the effectiveness of the proposed technique.

Both channel estimation and channel equalization carry out process on symbols. In order to distinguish channel estimation and channel equalization, symbol periods of channel estimation are described by taps. Throughout the article, superscripts $[\cdot]^T$ and $[\cdot]^H$ represent transpose and conjugate transpose, respectively.

II. SYSTEM STRUCTURE BASED ON THE ST-GAMP TECHNIQUE

A simple communication system is constructed, which is shown in Fig. 1. At the transmitter, information bits **b** are encoded, interleaved, and mapped by QPSK into symbols **s**. Then the training sequences **t** are linearly superimposed with the symbol sequences **s**, and the illustration of the superimposed training is shown in Fig. 2. Each data block is appended a cyclic prefix (CP) as a guard interval, and it is used to facilitate the frequency-domain equalization. At the receiver, after CP removal, the time-domain received signal **y** and the frequency-domain received signal $\mathbf{z}_1$ are obtained and used for three tasks: the first one is to obtain the initial channel estimates $\hat{\mathbf{h}}$ based on the LS algorithm with the ST scheme; the second one is to estimate the noise power $\hat{p}n$ based on **y** and $\hat{\mathbf{h}}$; the third one is to obtain the 'clean' received signal **z** for equalization, which equals to $\mathbf{z}_1$ minus the reconstructed training interference based on **t** and $\hat{\mathbf{h}}$. GAMP equalization is carried out based on $\hat{\mathbf{h}}$, $\hat{p}n$, and **z**, then turbo equalization, i.e., soft information exchange between the GAMP equalizer and the BCJR decoder, is performed iteratively, as shown in Fig. 3. The iterative process continues until a pre-set maximum number of iterations is reached. Turbo equalization is shown in Fig. 3. 1) Based on channel estimates $\hat{\mathbf{h}}$, noise power estimate $\hat{p}n$, and the 'clean' frequency-domain received signal **z**, GAMP equalization is performed, where the a priori, a posteriori, extrinsic means and variances are calculated. Then the soft outputs of the GAMP equalizer are converted into the extrinsic logarithm likelihood ratios (LLRs) of the interleaved coded bits, followed by deinterleaving and decoding. The outputs of the decoder are used by the GAMP equalizer and the channel estimator, therefore, there are two branches coming out of the BCJR decoder. Both of them use the latest decoding results (the LLRs of coded bits) of the BCJR decoder, which are updated in each iteration. In the first branch, the LLRs are interleaved, then input to the GAMP equalizer. In the second branch, hard decisions are performed on the estimated coded bits, which are interleaved, and mapped by QPSK into the estimated symbol sequences. They together with the training sequences, are used to get $\hat{\mathbf{h}}$. After that, based on the LLRs of the interleaved coded bits from the first branch, $\hat{\mathbf{h}}$, $\hat{p}n$, and **z** from the second branch, GAMP equalization is performed and the results are converted to the extrinsic LLRs, which are input to the decoder for the next round of turbo iteration.
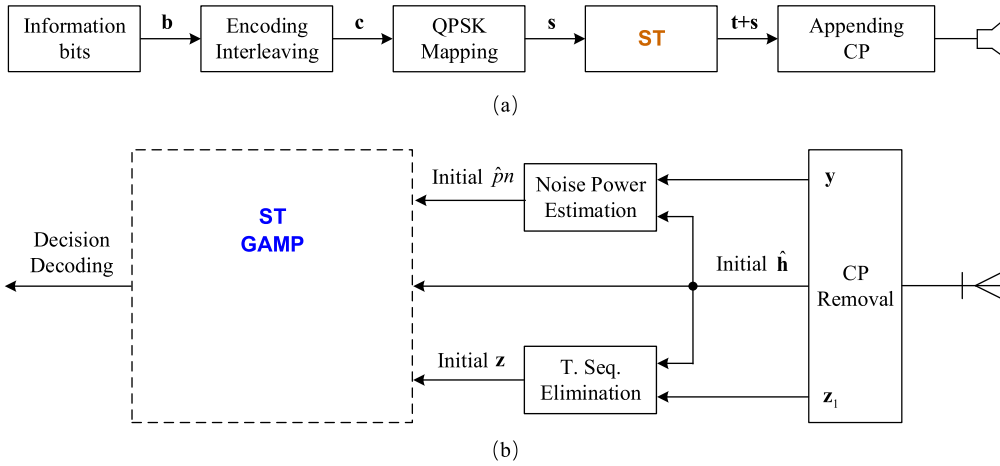
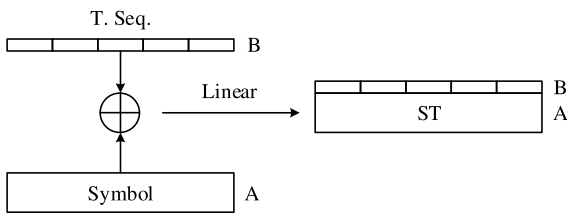FIGURE 1. Simple communication system. (a) Transmitter; (b) Receiver.

FIGURE 2. Illustration of the superimposed training.

III. PRINCIPLE OF THE ST-GAMP TECHNIQUE

A. CHANNEL ESTIMATION BASED ON THE ST SCHEME

The interleaved coded bits are denoted by $\mathbf{c}_n = \left[c_n^1, c_n^2, \cdots, c_n^Q\right]^T$, $c_n^q \in \{0, 1\}$. A symbol is denoted by $s_n \in \chi = \{\alpha_1, \alpha_2, \cdots, \alpha_{2Q}\}$ (Q is the number of the interleaved coded bits used to map into a symbol), where χ_q^0 and χ_q^1 represent all subsets of $\alpha_n = \left[\alpha_n^1, \alpha_n^2, \cdots, \alpha_n^Q\right]^T$. As QPSK mapping is used, $\alpha_n = \left[\alpha_n^1, \alpha_n^2\right]^T$, and $s_n \in 1/\sqrt{2}\{(1, -1), (1, 1), (-1, -1), (-1, 1)\}$. The transmitted signal consists of the symbol sequences denoted by $\mathbf{s} = [s_1, s_2, \cdots, s_{Ns}]^T$, and the training sequences denoted by $\mathbf{t} = [t_1, t_2, \cdots, t_{Ns}]^T$ with a period of T, which are generated using $t_k = e^{j\frac{\pi}{T}(k-1)^2}$, $k = 1, \cdots, T$ in [25]. The power ratio of the training sequences and the symbol sequences is denoted as r.

Take a data block with a length of Ns as an example. Due to the use of CPs, the channel matrix for the data block is a circulant one, denoted as $\mathbf{H}$, and the Gaussian white noise is denoted as $\mathbf{w}$. After CP removal, the received signal of the data block can be expressed as

$$\begin{aligned}\mathbf{y} &= \mathbf{H}(r\mathbf{t} + \mathbf{s}) + \mathbf{w} \\ &= \mathbf{Hs} + r\mathbf{Ht} + \mathbf{w}.\end{aligned} \tag{1}$$

Divide $\mathbf{y}$ into p segments, i.e., $\mathbf{y} = \left[\mathbf{y}_T, \mathbf{y}_{2T}, \cdots, \mathbf{y}_{pT}\right]^T$. The channel length is denoted as L, where $T \geq L$, then

the Toeplitz matrix formed by the training sequences can be represented as

$$\mathbf{A} = \begin{bmatrix} t_0 & t_{T-1} & \cdots & t_{T-L+1} \\ t_1 & t_0 & \cdots & t_{T-L+2} \\ \vdots & \vdots & \ddots & \vdots \\ t_{T-1} & t_{T-2} & \cdots & t_{T-L} \end{bmatrix}_{T \times L}. \tag{2}$$

Based on the LS algorithm, the channel estimates of the data block is obtained as

$$\hat{\mathbf{h}} = \left(\mathbf{A}^H \mathbf{A}\right)^{-1} \mathbf{A}^H \left\{\frac{1}{p}\sum_{i=1}^{p} \mathbf{y}_{iT}^T\right\}. \tag{3}$$

$\mathbf{F}$ is denoted as a standard discrete Fourier transform (DFT) matrix, and the (m, n)th element is given as $N^{-1/2}e^{-j2\pi mn/N}$, and $j = \sqrt{-1}$. $\mathbf{H}$ can be diagonalized by a DFT matrix, i.e.,

$$\mathbf{H} = \mathbf{F}^H \mathbf{D} \mathbf{F}, \tag{4}$$

where $\mathbf{D}$ is a diagonal matrix. From (1) and (4), the frequency-domain received signal can be obtained as

$$\mathbf{z}_1 = \mathbf{F}\mathbf{y} = \mathbf{F}\mathbf{F}^H \mathbf{D}\mathbf{F}(r\mathbf{t} + \mathbf{s}) + \mathbf{F}\mathbf{w}. \tag{5}$$

$\mathbf{F}$ is unitary, so

$$\mathbf{F}^H = \mathbf{F}^{-1}, \tag{6}$$

then we have

$$\mathbf{z}_1 = \mathbf{D}\mathbf{F}\mathbf{s} + r\mathbf{D}\mathbf{F}\mathbf{t} + \mathbf{F}\mathbf{w}. \tag{7}$$

The training interference elimination is carried out in frequency domain, i.e.,

$$\begin{aligned}\mathbf{z} &= \mathbf{z}_1 - \mathbf{F}\hat{\mathbf{h}}.*\mathbf{F}\mathbf{t} \\ &= \mathbf{D}\mathbf{F}\mathbf{s} + [\mathbf{D}(r\mathbf{F}\mathbf{t}) - \mathbf{F}\hat{\mathbf{h}}.*\mathbf{F}\mathbf{t} + \mathbf{F}\mathbf{w}] \\ &= \mathbf{D}\mathbf{F}\mathbf{s} + \mathbf{w}',\end{aligned} \tag{8}$$
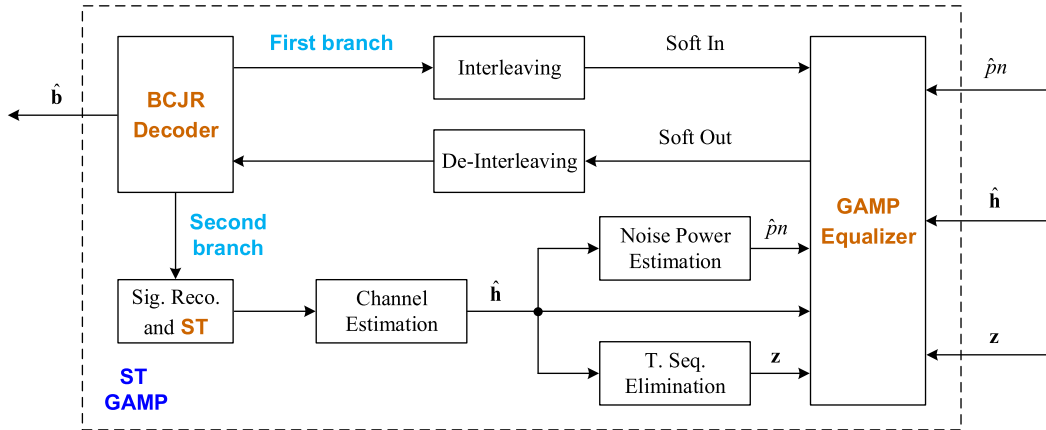
FIGURE 3. Turbo equalization.

where .* denotes the element-wise product of two vectors. For the 'clean' data block $\mathbf{z}$, we can estimate the diagonal matrix $\hat{\mathbf{D}}$ and diagonal elements of $\mathbf{D}$ as

$$\left[\hat{d}_1, \hat{d}_2, \cdots, \hat{d}_{N_s}\right]^T = \sqrt{N_s}\mathbf{F}\hat{\mathbf{h}}, \qquad (9)$$

which will be used for GAMP equalization. As the power of the transmitted symbols for the data block is 1, the noise power for the data block $\hat{p}n$ is the difference between the power of the received signal $P\mathbf{y}$ and the power of the channel energy $\left\|\hat{\mathbf{h}}\right\|^2$, i.e.,

$$\hat{p}n = P\mathbf{y} - \left\|\hat{\mathbf{h}}\right\|^2. \qquad (10)$$

B. LOW-COMPLEXITY FREQUENCY-DOMAIN CHANNEL EQUALIZATION BASED ON GAMP

Following [22]–[24], we compute the a priori, a posteriori, extrinsic means and variances of the symbols, and they are distinguished by superscripts a, p, and e, respectively. Initialization: Set extrinsic variance of a symbol $\mu_{r_n^e}^{-1} = 0$, extrinsic mean of a symbol $r_n^e = 0$, and a posterior mean of a symbol $\mathbf{s}^p = \mathbf{0}$.

Compute the mean m_n and the variance v_n for each s_n using the following equations

$$P_i = P^a \left(s_n = \alpha_i\right) \exp\left(-\mu_{r_n^e}^{-1}\left|\alpha_i - r_n^e\right|^2\right), \qquad (11)$$

$$P\left(s_n = \alpha_i\right) = \frac{P_i}{\sum_{i'=1}^{2^Q} P_{i'}}, \quad i = 1, 2, \cdots, 2^Q, \qquad (12)$$

$$m_n = \sum_{i=1}^{2^Q} \alpha_i P\left(s_n = \alpha_i\right), \qquad (13)$$

$$v_n = \sum_{i=1}^{2^Q} \left|\alpha_i - m_n\right|^2 P\left(s_n = \alpha_i\right), \qquad (14)$$

where $P^a\left(s_n = \alpha_i\right)$ represents the a priori probability of $s_n = \alpha_i$, which can be calculated based on the output LLRs from the decoder.

Compute the a priori variance $\mu_{p_n^a}$ and mean $\mathbf{p}^a$ as follows

$$\mu_{p_n^a} = \bar{v}\left|d_n\right|^2, \qquad (15)$$

$$\mathbf{p}^a = \hat{\mathbf{D}}\mathbf{F}\mathbf{m} - \Lambda_{\mathbf{p}^a}\mathbf{s}^p, \qquad (16)$$

where $\bar{v} = N_s^{-1}\sum_{n=1}^{N_s} v_n$, $\mathbf{m} = \left[m_1, m_2, \cdots, m_{N_s}\right]^T$ and $\Lambda_{\mathbf{p}^a} = \text{Diag}\left\{\mu_{p_1^a}, \mu_{p_2^a}, \cdots, \mu_{p_{N_s}^a}\right\}$.

Compute the a posterior variance $\mu_{s_n^p}$ and mean $\mathbf{s}^p$ as follows

$$\mu_{s_n^p} = \left(\hat{p}n + \mu_{p_n^a}\right)^{-1}, \qquad (17)$$

$$\mathbf{s}^p = \Lambda_{s^p}\left(\mathbf{z} - \mathbf{p}^a\right), \qquad (18)$$

where $\Lambda_{s^p} = \text{Diag}\left\{\mu_{s_1^p}, \mu_{s_2^p}, \cdots, \mu_{s_{N_s}^p}\right\}$.

Compute the extrinsic variance $\mu_{r_n^e}$ and mean $\mathbf{r}^e$ as follows

$$\mu_{r_1^e} = \mu_{r_2^e} = \cdots = \mu_{r_{N_s}^e} = N\left[\sum_{i=1}^{N_s}\left(\left|d_i\right|^2 \mu_{s_i^p}\right)\right]^{-1}, \qquad (19)$$

$$\mathbf{r}^e = \mathbf{m} + \mu_{r_1^e}\mathbf{F}^H\hat{\mathbf{D}}^H\mathbf{s}^p, \qquad (20)$$

where $\mathbf{r}^e = \left[r_1^e, r_2^e, \cdots, r_{N_s}^e\right]^T$. From (11) to (20), it is an inner iterative equalization, in order to reduce the computational amount of GAMP equalization, we incorporate the inner iteration into outer iteration between the GAMP equalizer and the BCJR decoder, that is, the inner iteration and the outer iteration are combined into one iteration. The computational complexity of GAMP equalization is only in the logarithmic order per symbol.

Combining the extrinsic mean and variance, we can obtain the extrinsic LLRs of α_n^1 and α_n^2 as follows

$$L^e\left(\alpha_n^1\right) = 2\sqrt{2}\,\text{Re}\left[r_n^e / \mu_{r_1^e}\right], \qquad (21)$$

$$L^e\left(\alpha_n^2\right) = 2\sqrt{2}\,\text{Im}\left[r_n^e / \mu_{r_1^e}\right]. \qquad (22)$$

The extrinsic LLRs are deinterleaved and decoded (BCJR). Then LLRs from the BCJR decoder are used for channel estimation, noise power estimation, and GAMP equalization for the next round of iteration.
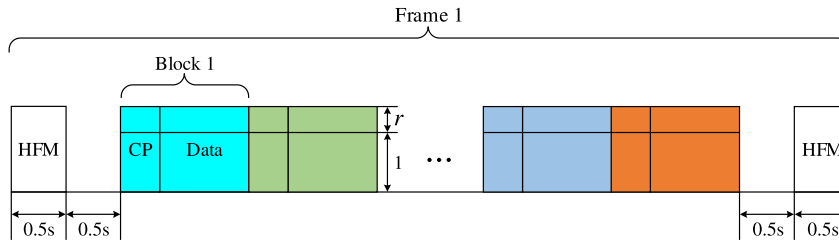
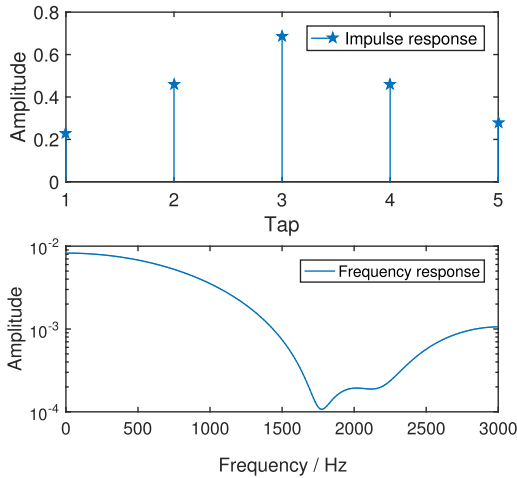**FIGURE 4.** Structure of the transmitted signal frame.

FIGURE 5. 5-order Proakis channel. (a) Impulse response; (b) Frequency response.

IV. SIMULATIONS AND EXPERIMENTS

Rate-1/2 nonsystematic convolutional code with generator $(5, 7)_8$, QPSK mapping, and the BCJR algorithm for decoding are used. The power ratio of the training sequences to the symbol sequences is set to 0.25:1. As the underwater acoustic channels can be very long, the length of CP is set to 512 symbol intervals. The structure of the transmitted signal frame is shown in Fig. 4. The hyperbolic frequency modulation (HFM) signals with negative and positive modulation rates, are employed respectively as the head and the tail of the signal frame to estimate and eliminate the average Doppler frequency offset, and synchronize the received signals [21].

In simulations, a baseband system is used, but it is noted that the low-pass filter is not employed. In experiments, a single carrier system was used, the center frequency, the bandwidth, the sampling frequency, and the symbol transmission rate were 12 kHz, 6 kHz, 96 kHz, and 4 ksym/s, respectively, and the band-pass filter was used.

A. BASEBAND SIMULATIONS

A static 5-order Proakis channel is used for all transmissions, as shown in Fig. 5. In each simulation, 120 blocks of information bits are used, and each block consists of 1024 information bits. Gaussian white noise is added to simulate the received signal with various signal to noise ratios (SNRs).
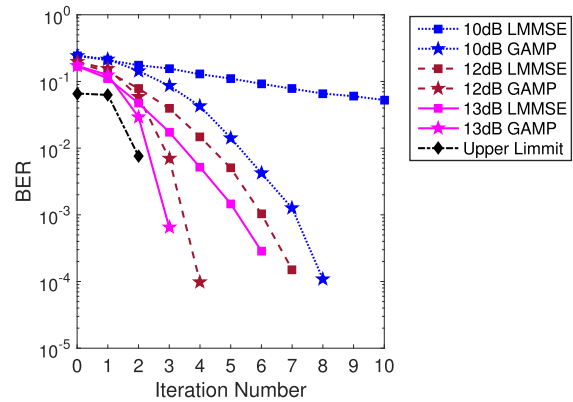

FIGURE 6. BER performance of the ST-GAMP technique.

We examine the performance of the ST-GAMP system in terms of the bit error rate (BER), and the corresponding BER performance is shown in Fig. 6. Black diamond curve represents the lower bound for the BER performance of the GAMP technique with SNR = 13 dB, where the time-multiplexed training scheme and the real 5-order Proakis channel are used. Star curves represent the BER performance of the ST-GAMP technique with different SNRs, and square curves represent the BER performance of the comparison technique with different SNRs, where the ST scheme and the linear minimum mean square error (LMMSE) equalization algorithm are combined to construct the ST-LMMSE technique. The BER performance of the ST-GAMP technique is significantly better than that of the ST-LMMSE technique. The pink star solid curve represents the BER performance of the ST-GAMP technique with SNR = 13 dB, and it can be seen that after 4 iterations, 120 blocks of information bits are correctly decoded, which verify that the proposed technique can effectively cope with harsh multi-path interference and Gaussian white noise.

B. COMMUNICATION EXPERIMENTS IN A POOL AND IN JIAOZHOU BAY IN 2019

A static communication experiment was carried out in a pool at Harbin Engineering University in January 2019. The horizontal distance between transceivers was about 7 m, and their deployment depths were random. The SNR was up to about 29 dB due to the short distance. The instantaneous channel in the pool is shown in Fig. 7(a).
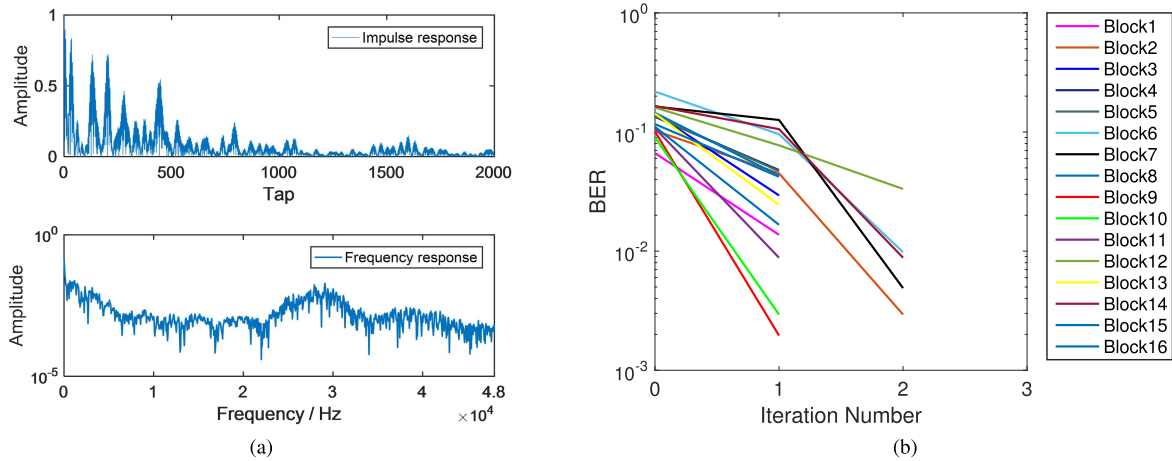
FIGURE 7. Channel in a pool and decoding performance. (a) Instantaneous channel; (b) BER of the ST-GAMP system versus the iteration number.
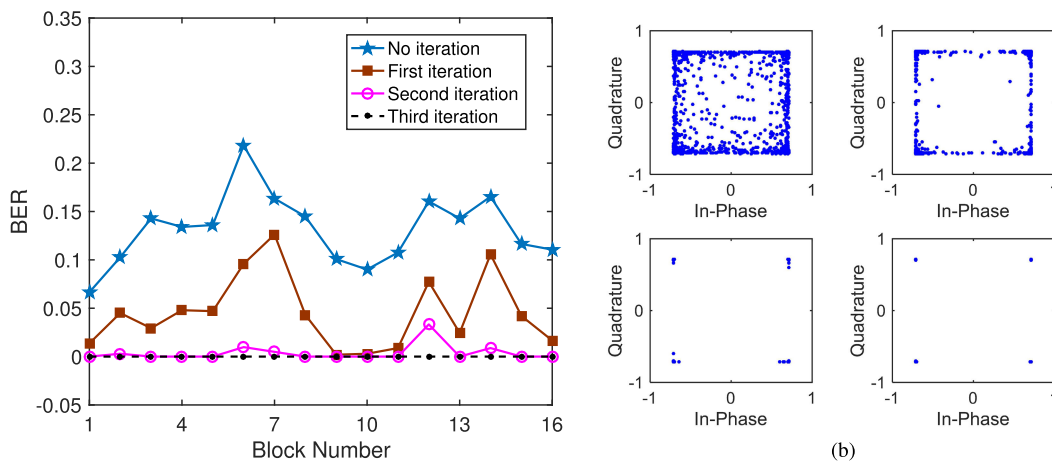

FIGURE 8. Decoding performance and constellation in a pool. (a) BER of the ST-GAMP system versus the block number; (b) Constellation plots of the 1st data block, and the iteration numbers are 0, 1, 2, and 3, respectively.
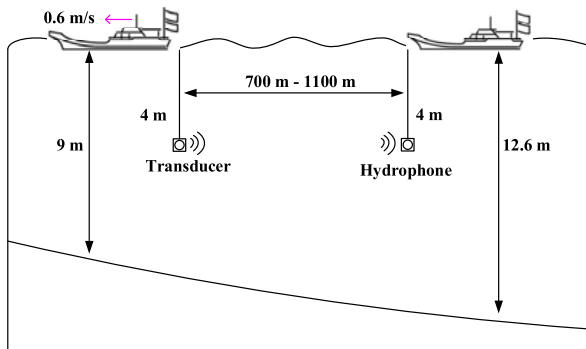

FIGURE 9. Experimental deployment.

The BER of the ST-GAMP system versus the iteration number is shown in Fig. 7(b), and the BER of the proposed system versus the block number is shown in Fig. 8(a), where it can be seen that, after 3 iterations, 16 blocks of information bits are decoded correctly, demonstrating the effectiveness

of the proposed system. We show the constellation of the estimated symbols of the 1st data block in Fig. 8(b) by using the ST-GAMP technique with various number of iterations, where it can be seen that, the constellation points are well clustered with only 3 iterations, indicating the excellent equalization performance of the proposed system.

Next, we examine the BER performance of the proposed system with moving transceivers. The experiments were conducted in Jiaozhou Bay in November 2019, and the experimental layout is shown in Fig. 9. The horizontal communication distance between the ships was 700 m - 1100 m, the ship with the hydrophone was anchored, but the ship with the transducer drifted away from it at a speed of about 0.6 m/s. The channel is shown in Fig. 10, where we can see from (b) that the channel changes considerably with time.

4 frames of information bits were transmitted to test the BER performance of the proposed system, where 1 frame contains 16 blocks, and each block is 1024 information bits. The BER performance is shown in Fig. 11(a), and it can be
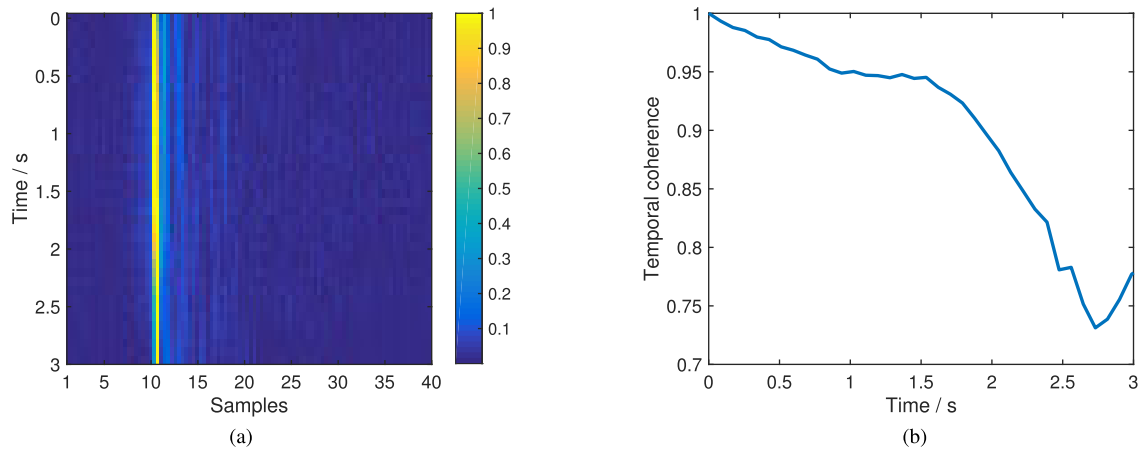
FIGURE 10. Channels in Jiaozhou Bay. (a) Waterfall plot; (b) Channel correlation curve.
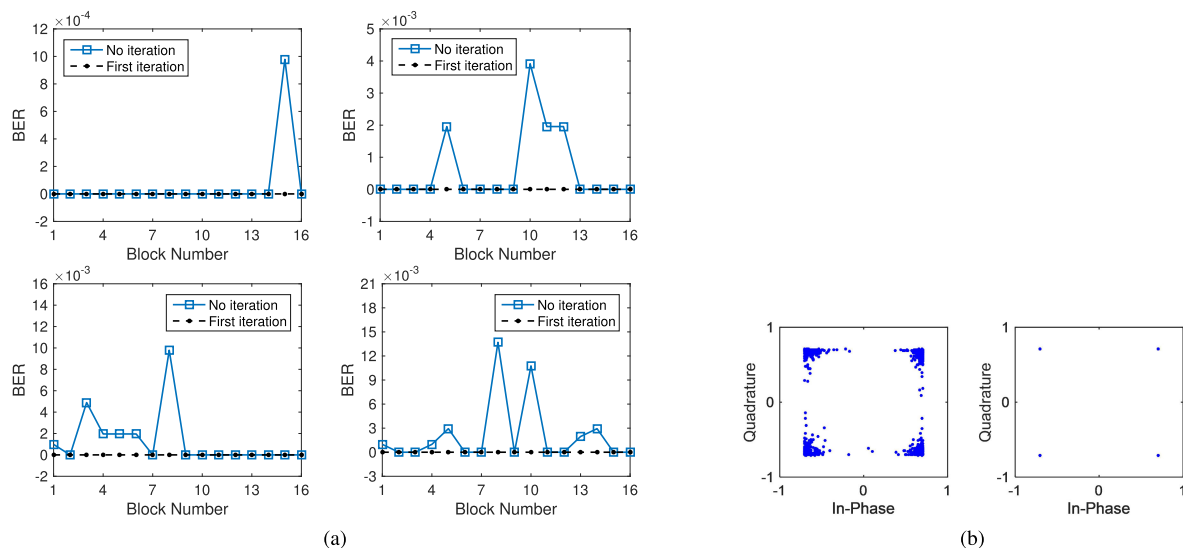

FIGURE 11. Decoding performance and constellation in Jiaozhou Bay. (a) Decoding performance of 4 frames; (b) Constellation plots of the 1st block of the 1st frame, and the iteration numbers are 0, and 1, respectively.

seen that from the results, after 1 iteration, all 4 frames of information bits are decoded correctly. Take the 1st block of the 1st frame to analyze the equalization performance, as shown in Fig. 11(b), and we can see that the estimated symbols are well clustered with only 1 iteration, demonstrating the effectiveness of the proposed system under the time-varying underwater acoustic channels.

V. CONCLUSION

We have addressed the issue of the channel estimation for the time-varying underwater acoustic channels with the ST scheme, where the training sequences are linearly superimposed with the symbol sequences, which only results in a small power loss, but the spectrum loss and the power loss caused by the traditional inserted training sequences are avoided. LS based channel estimation algorithm, with the superimposed training, has been proposed to realize the full potentials of the ST scheme. In particular, low-complexity

GAMP equalization algorithm has been proposed, which can be performed only in the complexity of a logarithmic order per symbol. The channel estimation, equalization and decoding have been performed jointly, which significantly improve the overall system performance. Simulations and experiments results have verified the effectiveness of the proposed technique.

REFERENCES

[1] A. Song, M. Stojanovic, and M. Chitre, "Editorial underwater acoustic communications: Where we stand and what is next?" *IEEE J. Ocean. Eng.*, vol. 44, no. 1, pp. 1–6, Jan. 2019.

[2] T. C. Yang, "Properties of underwater acoustic communication channels in shallow water," *J. Acoust. Soc. Amer.*, vol. 131, no. 1, pp. 129–145, Jan. 2012.

[3] P. Qarabaqi and M. Stojanovic, "Statistical characterization and computationally efficient modeling of a class of underwater acoustic communication channels," *IEEE J. Ocean. Eng.*, vol. 38, no. 4, pp. 701–717, Oct. 2013.

[4] C. R. Berger, S. Zhou, J. C. Preisig, and P. Willett, "Sparse channel estimation for multicarrier underwater acoustic communication: From subspace methods to compressed sensing," *IEEE Trans. Signal Process.*, vol. 58, no. 3, pp. 1708–1721, Mar. 2010.

[5] J. Huang, S. Zhou, J. Huang, C. R. Berger, and P. Willett, "Progressive inter-carrier interference equalization for OFDM transmission over time-varying underwater acoustic channels," *IEEE J. Sel. Topics Signal Process.*, vol. 5, no. 8, pp. 1524–1536, Dec. 2011.

[6] Z. Wang, S. Zhou, J. C. Preisig, K. R. Pattipati, and P. Willett, "Clustered adaptation for estimation of time-varying underwater acoustic channels," *IEEE Trans. Signal Process.*, vol. 60, no. 6, pp. 3079–3091, Jun. 2012.

[7] F. Qu, X. Nie, and W. Xu, "A two-stage approach for the estimation of doubly spread acoustic channels," *IEEE J. Ocean. Eng.*, vol. 40, no. 1, pp. 131–143, Jan. 2015.

[8] X. Qin, F. Qu, and Y. Rosa Zheng, "Bayesian iterative channel estimation and turbo equalization for multiple-input–multiple-output underwater acoustic communications," *IEEE J. Ocean. Eng.*, vol. 46, no. 1, pp. 326–337, Jan. 2021.

[9] Z. Yang and Y. Rosa Zheng, "Iterative channel estimation and turbo equalization for multiple-input multiple-output underwater acoustic communications," *IEEE J. Ocean. Eng.*, vol. 41, no. 1, pp. 232–242, Jan. 2016.

[10] Y.-H. Zhou, F. Tong, and G.-Q. Zhang, "Distributed compressed sensing estimation of underwater acoustic OFDM channel," *Appl. Acoust.*, vol. 117, pp. 160–166, Feb. 2017.

[11] Y.-H. Zhou, W.-H. Jiang, F. Tong, and G.-Q. Zhang, "Exploiting joint sparsity for underwater acoustic MIMO communications," *Appl. Acoust.*, vol. 116, pp. 357–363, Jan. 2017.

[12] Y. Zhou, A. Song, F. Tong, and R. Kastner, "Distributed compressed sensing based channel estimation for underwater acoustic multiband transmissions," *J. Acoust. Soc. Amer.*, vol. 143, no. 6, pp. 3985–3996, Jun. 2018.

[13] G. Qiao, Q. Song, L. Ma, and L. Wan, "A low-complexity orthogonal matching pursuit based channel estimation method for time-varying underwater acoustic OFDM systems," *Appl. Acoust.*, vol. 148, pp. 246–250, May 2019.

[14] A. Tadayon and M. Stojanovic, "Iterative sparse channel estimation and spatial correlation learning for multichannel acoustic OFDM systems," *IEEE J. Ocean. Eng.*, vol. 44, no. 4, pp. 820–836, Oct. 2019.

[15] J. Yin, W. Ge, X. Han, and L. Guo, "Frequency-domain equalization with interference rejection combining for single carrier multiple-input multiple-output underwater acoustic communications," *J. Acoust. Soc. Amer.*, vol. 147, no. 2, pp. EL138–EL143, Feb. 2020.

[16] A. Yellepeddi and J. C. Preisig, "Adaptive equalization in a turbo loop," *IEEE Trans. Wireless Commun.*, vol. 14, no. 9, pp. 5111–5122, Sep. 2015.

[17] J. Xi, S. Yan, L. Xu, Z. Zhang, and D. Zeng, "Frequency–time domain turbo equalization for underwater acoustic communications," *IEEE J. Ocean. Eng.*, vol. 45, no. 2, pp. 665–679, Apr. 2020.

[18] C. He, L. Jing, R. Xi, H. Wang, F. Hua, Q. Dang, and Q. Zhang, "Time-frequency domain turbo equalization for single-carrier underwater acoustic communications," *IEEE Access*, vol. 7, pp. 73324–73335, 2019.

[19] J. Han, S. P. Chepuri, Q. Zhang, and G. Leus, "Iterative per-vector equalization for orthogonal signal-division multiplexing over time-varying underwater acoustic channels," *IEEE J. Ocean. Eng.*, vol. 44, no. 1, pp. 240–255, Jan. 2019.

[20] J. Xi, S. Yan, and L. Xu, "Direct-adaptation based bidirectional turbo equalization for underwater acoustic communications: Algorithm and undersea experimental results," *J. Acoust. Soc. Amer.*, vol. 143, no. 5, pp. 2715–2728, May 2018.

[21] K. Pelekanakis and M. Chitre, "Robust equalization of mobile underwater acoustic channels," *IEEE J. Ocean. Eng.*, vol. 40, no. 4, pp. 775–784, Oct. 2015.

[22] Q. Guo, D. Huang, S. Nordholm, J. Xi, and Y. Yu, "Iterative frequency domain equalization with generalized approximate message passing," *IEEE Signal Process. Lett.*, vol. 20, no. 6, pp. 559–562, Jun. 2013.

[23] Q. Guo and D. D. Huang, "A concise representation for the soft-in soft-out LMMSE detector," *IEEE Commun. Lett.*, vol. 15, no. 5, pp. 566–568, May 2011.

[24] Q. Guo, L. Ping, and D. Huang, "A low-complexity iterative channel estimation and detection technique for doubly selective channels," *IEEE Trans. Wireless Commun.*, vol. 8, no. 8, pp. 4340–4349, Aug. 2009.

[25] A. G. Orozco-Lugo, M. M. Lara, and D. C. McLernon, "Channel estimation using implicit training," *IEEE Trans. Signal Process.*, vol. 52, no. 1, pp. 240–254, Jan. 2004.

GUANG YANG was born in 1981. He received the Ph.D. degree from Harbin Engineering University, in 2016. From 2014 to 2016, he was a Visiting Scholar with the University of Western Australia. He is currently an Assistant Professor with the School of Information and Control Engineering, Qingdao University of Technology, China. In 2020, he got a Postdoctoral position from the University of Western Australia. His interests include moving underwater acoustic communications and estimation and equalization of fast time-varying underwater acoustic channels.

TAILIAN LIU was born in 1983. He received the Ph.D. degree from the Institute of Modern Physics, University of Chinese Academy of Sciences, in 2012. He is currently an Assistant Professor with the College of Science and Information, Qingdao Agricultural University, China. His research interests include communication protocol and the Internet of Things.
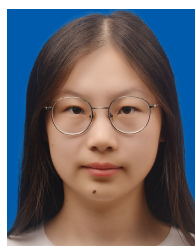
HANXUE DING was born in 1998. She received the B.Eng. degree in information and control engineering from the Qingdao University of Technology, Qingdao, China, in 2020. She is currently pursuing the master's degree in electronic and information engineering with Beijing Jiaotong University, Beijing, China. Her research interest includes underwater acoustic communications.
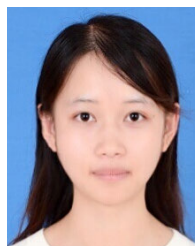
QI YAN was born in 1996. She received the B.Eng. degree in electronic and information engineering from the lnner Mongolia University of Science and Technology, China, in 2019. She is currently pursuing the M.Eng. degree in information and communication engineering with the Qingdao University of Technology, China. Her research interest includes underwater acoustic communications.

XINJIE WANG was born in 1980. He received the Ph.D. degree in computer application technology from the Ocean University of China, China, in 2016. Since 2021, he has been an Associate Professor with the School of Information and Control Engineering, Qingdao University of Technology, China. His research interests include cognitive radio networks, physical layer security, energy harvesting, drone communications, and underwater acoustic communication.

• • •